Atmospheric Carbon Tetrafluoride: A Nearly Inert Gas

Abstract. *An analysis of existing thermodynamic, photochemical, and kinetic data indicates that the dominant sinks for atmospheric carbon tetrafluoride (CF_4) are in and above the mesosphere. Theoretical calculations predict an atmospheric residence time for CF_4 of over 10,000 years, about 100 times that for dichlorodifluoromethane (CF_2Cl_2) and monofluorotrichloromethane ($CFCl_3$). It is predicted that CF_4 will be well mixed through the stratosphere and mesosphere; only one or two parts of hydrogen fluoride in 10^{12} are predicted in the high stratosphere as a result of the decomposition of CF_4. Although natural sources of CF_4 cannot be ruled out, there are several likely industrial sources that may account for its present concentration. The principal environmental effect of CF_4 could be the trapping of outgoing planetary infrared energy in its intense bands near 8 micrometers.*

Carbon tetrafluoride (CF_4) was detected in the air of several European countries by Gassman in 1973 (*1*) and in both hemispheres of the troposphere by Rasmussen *et al.* (*2*) in 1978. This compound is probably the most stable fluorocarbon gas. In this report I examine the potential of atmospheric and environmental processes to decompose CF_4 and conclude that it has an atmospheric lifetime of over 10^4 years. Its principal sinks are vacuum ultraviolet (UV) radiation in the high mesosphere and ionosphere, possible (but unlikely) reactions with electronically excited oxygen atoms and with vibrationally excited ($v = 9$) OH molecules in the stratosphere and above, several ionospheric processes, and pyrolysis in high-temperature combustion. Its dominant sources are uncertain, but I identify several likely industrial processes. Such a long lifetime (residence time) ensures that relatively small sources will increase the atmospheric CF_4 burden and that CF_4 will remain ubiquitous in the atmosphere.

In an effort to understand the atmospheric behavior of CF_4 as quantitatively as possible, I have used available data on its chemical properties, estimated certain unknown parameters, and performed numerical calculations to simulate its atmospheric transport and photochemistry. Table 1 lists possible CF_4 sinks and the reaction rate parameters I adopted. Solar vacuum UV photons with wavelength $\lambda < 103$ nm photodissociate and photoionize CF_4 (*3*). Although no absorption has been observed for $\lambda > 103$ nm (*3*), I have performed calculations with photodissociation cross sections, σ, of 3×10^{-19} and 3×10^{-20} cm^2 at $\lambda = 122$ nm because of the intense solar 121.6-nm line and with σ (122 nm) = 0. These data yield photodissociation rates, J (per second) as follows (*3*): the total J above the entire atmosphere (altitude, $z = \infty$) is 6.8×10^{-7} due to absorption over all wavelengths, that is, 122 nm and 60 nm $< \lambda <$ 103 nm. With the maximum σ at 122 nm, that is, 3×10^{-19} cm^2, J (122 nm) = 10^{-7} at $z = \infty$. As a result of absorption by O_2 and N_2, the only significant photodissociation below an altitude of 90 km is due to the solar lines at 122 and 103 nm. With the maximum σ, J (122 nm) = 4.7×10^{-8}, 2.6×10^{-8}, 1.5×10^{-9}, and 3.6×10^{-14} at 90, 80, 70, and 60 km, respectively, when averaged diurnally; J (103 nm) = 9×10^{-9}, 3×10^{-11}, and 1.2×10^{-23} at $z = \infty$, 90, and 80 km, respectively. Consequences of these rates are discussed below.

Chemical reactions between CF_4 and atmospheric constituents are limited by C-F bond strengths. I estimated upper-limit bimolecular rate constants k_1 through k_{13} (Table 1) as follows. Reaction 1, an O atom insertion, should be slower than the observed (upper limit) rate (*4*) for O + CF_3H, an H abstraction. I assumed an Arrhenius expression of the form $A \exp(-E_a/RT)$, where A is a constant, E_a is the activation energy, R is the gas constant, and T is the temperature. For a generous upper limit on k_1, I took E_a for O + CF_3H and O + CF_4 as their respective ΔH (enthalpy of reaction) values (*5*), although generally $E_a > \Delta H$. Multiplying this maximum k_1 by concentrations of O at each altitude from 10 to 110 km, one finds that the maximum product, 10^{-11} sec^{-1}, occurs near the stratopause (50 km) (*6*).

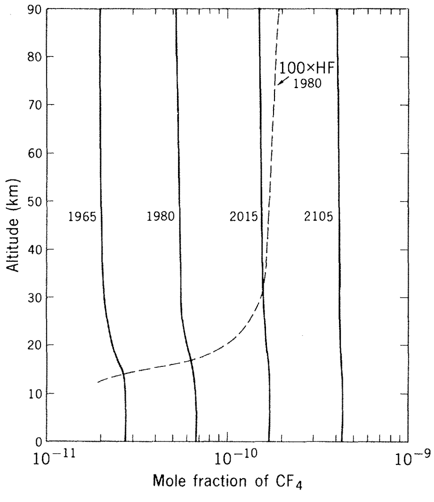

Fig. 1. Predicted altitude profiles for the mole fraction of CF_4 in the years 1965, 1980, 2015, and 2105 for the case when the sinks of Table 1 are presumed effective at their upper limit rates. The ground-level source of CF_4 was assumed to begin in 1935 at 5.7×10^9 g year^{-1} increasing (at about 6 percent per year) to 4.8×10^{10} g year^{-1} in 1975 and remaining constant thereafter at the 1975 rate. The 1980 profie approximates available data (*1*, *2*). Eventually, the CF_4 mole fraction would rise to 4×10^{-8}. Also shown is (100 times) the predicted 1980 HF profile due to CF_4 decomposition.

The only exothermic reaction of CF_4 with $O(^1D)$ other than quenching to $O(^3P)$ is the insertion reaction in Table 1; for $O(^1S)$, two exothermic paths exist. In my calculations I let k_4, k_5, and k_6 = 0 and 10^{-12} cm^3 sec^{-1} separately (*7*). Reaction with H atoms, although exothermic, requires at least 10 kcal per mole of activation energy (*8*). Reactions of ground-state OH with CF_4 are strongly endothermic and thus negligible. Vibrationally excited OH ($v = 1, 2, \cdots 9$) is present in the stratosphere and mesosphere (*9*). It is possible for CF_4 to react with OH ($v = 9$); I estimated reaction rates k_{11} and k_{12} in Table 1. Dissociative electron capture by CF_4 is strongly endothermic (*10*) so that free electrons in the lower ionosphere are insignificant. Above 150 km ionospheric photoelectrons with energies > 2 eV would dissociate CF_4, but this process would be very slow globally because the CF_4 available for attack there is 10^{-9} of that in the troposphere.

The nonphotochemical processes in Table 1 were evaluated as follows. If all rainfall is saturated with CF_4 with respect to its atmospheric partial pressure, pCF_4, and 1 m of water falls annually, the ratio of annually precipitated CF_4 to the atmospheric content is 2×10^{-6} for any pCF_4, according to its solubility (*5*). Moreover, because the rate of hydrolysis of CF_4 is immeasurably small (*11*), the capacity of the oceans to assimilate CF_4 is limited by its solubility; if all ocean waters (surface and deep) were saturated with CF_4, less than 0.2 percent of the atmospheric burden of CF_4 at any time would be in the oceans. The removal time due to pyrolysis in Table 1 is based on annual O_2 consumption rates in high-temperature combustion (*11*). Finally, there are no indications of biological processes that can break C-F bonds in CF_4 (*12*).

With the photochemical reactions of Table 1, I performed numerical calculations (*13*) for the time and altitude dependence of CF_4 concentrations. A constant ground-level source of CF_4 natural-

0036-8075/79/1005-0059$00.50/0

Table 1. Bimolecular rate constants (in cubic centimeters per second) and process rates for the decomposition of atmospheric CF_4. Additional reactions between CF_4 and NO, NO_2, CO, O_3, HO_2, SO_2, Cl, ClO, HCl, other gases, and positive ions were considered but no exothermic paths exist. Although the reaction $H_2 + CF_4 \rightarrow HF + CF_3H$ is exothermic, it is expected to have a prohibitive activation energy as is the case for $NO_3 + CF_4 \rightarrow NO_2 + CF_3OF$. Other natural sinks, for example, solar x-rays, ionospheric photoelectrons, lightning discharges, and surface reactions with atmospheric aerosols are active but unimportant quantitatively (*11*).

Candidate reaction or process	ΔH_{298} (kcal mole^{-1})	Adopted reaction rate parameter	Reference
Vacuum UV photodissociation	Bond dissociation energy is 129 kcal mole^{-1} (λ = 220 nm)	$\sigma(\lambda)$ for $\lambda < 103$ nm σ (121 nm) $< 3 \times 10^{-19}$ cm^2	(*3*) (*3*)
$O + CF_4 \rightarrow CF_2O + F_2$	+10.8	$k_1 < 2.0 \times 10^{-13} \exp(-5000/T)$	(*4, 5, 7*)
$O + CF_4 \rightarrow FO + CF_3$	+77.1	$k_2 = 0.0$	(*4-6*)
$O + CF_4 \rightarrow CO + 2F_2$	+137.1	$k_3 = 0.0$	(*4-6*)
$O(^1D) + CF_4 \rightarrow CF_2O + F_2$	−34.4	$k_4 = 0.0, k_4 = 10^{-12}$	(*5-7*)
$O(^1S) + CF_4 \rightarrow FO + CF_3$	−19.1	$k_5 = 0.0, k_5 = 10^{-12}$	(*5-7*)
$O(^1S) + CF_4 \rightarrow F_2 + CF_2O$	−85.4	$k_6 = 0.0, k_5 = 10^{-12}$	(*5-7*)
$H + CF_4 \rightarrow HF + CF_3$	−6.6	$k_7 < 3.0 \times 10^{-11} \exp(-5000/T)$	(*8*)
$OH + CF_4 \rightarrow FO + CF_3H$	+73.0	$k_8 = 0.0$	(*5*)
$OH + CF_4 \rightarrow HOF + CF_3$	+70.2	$k_9 = 0.0$	(*5*)
$OH + CF_4 \rightarrow$ other products	>+77	$k_{10} = 0.0$	(*5*)
$OH^* (v=9) + CF_4 \rightarrow FO + CF_3H$	−3.1 ± 10	$k_{11} \leq 10^{-12}$	(*6*)
$OH^* (v=9) + CF_4 \rightarrow HOF + CF_3$	−5.9 ± 10	$k_{12} \leq 10^{-11}$	(*6*)
Thermal $e + CF_4 \rightarrow F^- + CF_3$	+50	$k_{13} \leq 5.0 \times 10^{-7} \exp(-25{,}000/T)$	(*10*)
Rainout in the troposphere		Removal time, 500,000 years	(*11*)
Biospheric or microbiological consumption		None	(*12*)
Pyrolysis in high-temperature combustion		Removal time, > 50,000 years	(*11*)

ly leads to an eventual steady-state atmospheric equilibrium vertical concentration profile. A source of 2.4×10^{10}g year^{-1} (10^6 cm^{-2} sec^{-1}) gives a steady-state CF_4 concentration, f_s (mole fraction), of 20 parts per billion (ppb) (2×10^{-8}) when all photochemical losses are maximized as in Table 1. In this case the atmospheric residence time, τ, defined as (total atmospheric CF_4 content)/(CF_4 input flux), is 14,000 years. With the same source and maximum photodissociation but $k_1, k_2, \ldots k_{13} = 0$, τ = 38,000 years and f_s = 56 ppb. When σ (122 nm) = 3×10^{-20} cm^2, that is, 0.1 times maximum photodissociation and $k_1, k_2, \ldots k_{13}$ are maximized, τ = 23,000 years and f_s = 34 ppb. Taking σ (122 nm) = 0 and $k_1, k_2, \ldots k_{13} = 0$, one finds $\tau = 17 \times 10^6$ years, but this is unrealistic because nonphotochemical processes such as combustion would limit the CF_4 residence time (at least until fossil fuels are depleted).

I also performed calculations in which a time-varying, presumably industrial CF_4 source was used. Figure 1 shows altitude profiles of the CF_4 mole fraction at four dates. All photochemical destruction rates for CF_4 in Fig. 1 were the maximum values of Table 1. The present atmospheric burden of CF_4, about 10^{12} g (mole fraction = 6×10^{-11}), could have materialized thus. Because the CF_4 sinks are in the mesosphere and above except for $O(^1D)$ and OH* (minor compared to 122-nm photodissociation), only about 10^{-3} to 10^{-2} of the atmospheric CF_4 is exposed to the sinks at any time. The local photochemical removal processes have characteristic time constants of over 100 years, and τ = 14,000 years. Thus the CF_4 concentration increases with time, and the altitude profile approaches a straight line. At steady state, the ratio of the 90-km mole fraction to the 0-km mole fraction is 0.97. Thus the release of four F atoms in CF_4 decomposition leads to very little HF (Fig. 1). The dominant inorganic F compound in the stratosphere and mesophere should be HF (*14*). If CF_4 is a recent addition to the air, its mole fraction, f, will be less in the stratosphere and above than at $z = 0$, for example, the 1980 profile in Fig. 1. If, instead, CF_4 was injected into the air over 100 years ago, it should be well mixed (like the A.D. 2105 profile). In any case, an atmospheric residence time of > 14,000 years implies that, even with no sources, a given CF_4 profile will decay by only 7 percent in 1000 years ($e^{-1/14}$), as I have confirmed by additional numerical computations.

With such a long atmospheric lifetime, CF_4 concentrations will grow because CF_4 has industrial sources, for example, CF_4 released in the electrolytic reduction of alumina (*15*). Indeed, the liberation of CF_4 is not entirely limited to relatively brief anode-effect intervals. Japanese studies (*15*) suggest that the estimate of Rasmussen *et al.* (*2*) of 6×10^9 g of CF_4 per year released during electrolytic cell anode effects are supplemented by CF_4 released during normal cell operation. Release of as much as 10^{10} g year^{-1} is easily possible, but changing industrial practices, technology, and output imperil such estimates; direct measurements are needed. Several other industrial processes are likely sources of CF_4, either because CF_4 has been detected in the process or because C, F, and heat are available: the electrolytic generation of F_2, especially in carbon or graphite electrode systems, the analogous reduction of UF_4 or UF_6 (*16*), the use of fluorspar in steelmaking (*17*, p. 298; *18*) (although CF_4 production from CaF_2 seems disfavored thermodynamically), the burning of polyfluoroethylenes, rocket fuel combustion (*18*), and inadvertent production in fluorocarbon manufacture. Direct, intentional industrial production of CF_4 amounts to only 10 to 60 tons per year.

Sources of CF_4, especially anthropogenic, require measurements to quantify, as does the possible CF_4 photoabsorption at 122 nm. With these data, more accurate predictions of CF_4 concentrations and effects will be feasible.

Note added in proof: A recent stratospheric measurement by Goldman *et al.* (*19*) found 7.5×10^{-11} (mole fraction CF_4) at 25 km, as is roughly predicted by the curve for 1980 in Fig. 1.

RALPH J. CICERONE
Scripps Institution of Oceanography,
University of California, San Diego,
La Jolla 92093

References and Notes

1. M. Gassman, *Naturwissenschaften* **61**, 127 (1974).
2. R. Rasmussen, S. Penkett, N. Prosser, *Nature (London)* **277**, 549 (1979).
3. G. Cook and B. Ching [*J Chem. Phys.* **43**, 1974 (1965)] and P. Sauvageau, R. Gilbert, P. Berlow, and C. Sandorfy [*ibid.* **59**, 762 (1973)] give CF_4 photoabsorption data for $60 < \lambda < 103$ nm. Absorption for $\lambda > 105$ nm reported by J. Dacey and J. Hodgins [*Can J. Res. Sect. B* **28**, 173 (1950)] and by G. Moe and A. Duncan [*J. Am. Chem. Soc.* **74**, 3140 (1952)] was due to impurities; see C. Zobel and A. Duncan [*ibid.* **77**, 2611 (1955)] and L. Edwards and J. Raymonda

[*ibid.* **91**, 5937 (1969)]. From the experimental sensitivity of Edwards and Raymonda, I concluded that σ (122 nm) $< 3 \times 10^{-19}$ cm^2. Electron impact and photoelectron spectra and the theoretical spectroscopy of CF_4 show no significant absorption bands for $\lambda > 99$ nm [C. Sandorfy, *Atmos. Environ.* **10**, 343 (1976); W. Harshbarger and E. Lassettre, *J. Chem. Phys.* **58**, 1505 (1973); R. Robin, in *Higher Excited States of Polyatomic Molecules* (Academic Press, New York, 1974), vol. 1, pp. 178–191]. To compute CF_4 photodissociation rates, I used solar irradiances from J. Timothy [in *The Solar Output and Its Variation*, O. White, Ed. (Colorado Univ. Press, Boulder, 1977), pp. 237–258].

4. W. Wilson, Jr., and J. O'Donovan, *J. Chem. Phys.* **48**, 2829 (1968). One might also deduce an upper limit for k_1 from the analogous but exothermic insertion into CCl_4 measured by A. Ung and H. Schiff [*Can. J. Chem.* **40**, 486 (1962)]; I obtain $k_1 < 3 \times 10^{-14} \exp(-7250/T)$, that is, smaller than the k_1 in Table 1.
5. Molecular enthalpies for calculating reaction enthalpies were taken from the *Joint Army-Navy-Air Force Thermochemical Tables* (National Bureau of Standards, Gaithersburg, Md., ed. 2, 1971). *The Handbook of Chemistry and Physics* (CRC Press, Cleveland, ed. 58, 1978) erroneously gives $\Delta H^0_{f298} = -162$ kcal mole^{-1} for CF_4 instead of the correct value, -223 kcal mole^{-1}. The *Handbook of Chemistry and Physics* did provide a solubility of CF_4 in water at 25°C of 1.5×10^{-5} (by weight), however.
6. Temperature, N_2 profiles, and O_2 profiles are from *The U.S. Standard Atmosphere* (National Oceanic and Atmospheric Administration, Washington, D.C., 1976). Profiles of O, O(^1D), and H are from S. C. Liu and R. Cicerone's unpublished calculations; OH* and O(^1S) values are from A. Nagy, S. Liu, and D. Baker [*Geophys. Res. Lett.* **3**, 731 (1976)] and T. Donahue, B. Guenther, and R. Thomas [*J. Geophys. Res.* **78**, 6662 (1973)], respectively.
7. Insertion of O into C-F bonds is less likely than for O into CH_4, but the only experimental upper limit on k_4 is 10^{-11} cm^3 sec^{-1} [from R. Atkinson, G. Breuer, J. Pitts, Jr., H. Sandoval, *J. Geophys. Res.* **81**, 5765 (1976)]. I chose k_4, k_5, and $k_6 \leq 10^{-12}$ cm^3 sec^{-1} based on the work of K. Schofield [*J. Photochem* **9**, 55 (1978)] and on discussions with K. Schofield and W. DeMore.
8. For $H + CF_4 \rightarrow HF + CF_3$, E_a must be larger than the value of 9.5 kcal mole^{-1} found for similar reactions with CH_3Cl and CH_3F by A. Westenberg and N. deHaas [*J. Chem. Phys.* **62**, 3321 (1975)]. Similarly, for $H + CF_3Cl \rightarrow HCl + CF_3$, J. Bradley, D. Whytock, and T. Zaleski [*J. Chem. Soc. Faraday Trans. 1* **72**, 2284 (1974)] found $E_a = 8.8$ kcal mole^{-1}. Even higher E_a values can be gleaned from Dacey and Hodgins in (*3*) and from V. Kochubei and F. Moin [*Kinet. Catal.* **11**, 712 (1970)].
9. G. Streit and H. Johnston, *J. Chem. Phys.* **64**, 95 (1978).
10. For a C-F bond energy of 129 kcal mole^{-1} (5.61 eV), $e + CF_4 \rightarrow F^- + CF_3$ is endothermic by 2.27 eV because the electron affinity of F is 3.34 eV [from H. Hotop and W. Lineberger, *J. Phys. Chem. Ref. Data* **4**, 539 (1975)]. By contrast, $e + CFCl_3 \rightarrow Cl^- + CFCl_2$ is exothermic by 0.2 eV.
11. Hydrolysis of perhalocarbons, pyrolysis in high-temperature combustion, dissociation by lightning, and reaction on atmospheric aerosols are discussed in *Halocarbons: Effects on Stratospheric Ozone* (National Academy of Sciences, Washington, D.C., 1976), pp. 179–201; CF_4 is stable at temperatures of at least 1200°C [see (*17*, p. 310)].
12. F. Letkiewicz, *Report EPA-560/8-76-003* (Environmental Protection Agency, Washington, D.C., 1976), pp. 72–73. Although certain African plants can cleave single C-F bonds [R. Hall and R. Cain, *New Phytol.* **71**, 839 (1972)], no known marine natural product contains C-F bonds [J. Faulkner, *Tetrahedron* **33**, 1421 (1977)].
13. The spatial one-dimensional, time-dependent partial differential equation of mass transport with photochemical loss was solved by Crank-Nicolson finite-differencing with $\Delta z = 1$ km and $\Delta t = 30$ days. Eddy-mixing coefficients were from D. Hunten [*Profile A in Chlorofluoromethanes in the Stratosphere* (National Aeronautics and Space Administration, Washington, D.C., 1977), p. 137]. Boundary conditions were as follows: at $z = 0$, a CF_4 input flux was either time-varying as specified in the text, constant for a steady-state calculation, or 0 when an initial CF_4 profile was allowed to decay as a result of sinks; at $z = 90$ km, the upward CF_4 flux is equal to the integrated loss above 90 km from the previous time step. Integrations of 300 years conserved mass to better than 1 percent as did steady-state calculations.
14. R. Stolarski and R. Rundel, *Geophys. Res. Lett.* **2**, 443 (1975); R. Watson, P. Smokler, W. DeMore, *Publication 77-181* (Jet Propulsion Laboratory, Pasadena, Calif., 1977).
15. N. Kameyama, T. Somiya, S. Nagaura, Y. Konishi, paper presented at the 12th International Congress on Pure and Applied Chemistry, New York, 1951; J. Henry and R. Holliday, *J. Met.* **9**, 1384 (1957); T. Somiya and Y. Konishi, *Kogakuin Univ. Res. Rep. 30* (1971), p. 72.
16. C. Slesser and S. Schram, Eds., *Preparation, Properties, and Technology of Fluorine and Organic Fluoro Compounds* (McGraw-Hill, New York, 1951), pp. 31–112; J. Katz and E. Rabinowitch, *The Chemistry of Uranium* (McGraw-Hill, New York, 1951), pp. 126 and 442.
17. H. G. Bryce, in *Fluorine Chemistry*, J. Simons, Ed. (Academic Press, New York, 1964), vol. 5.
18. A. Cottrell, *An Introduction to Metallurgy* (St. Martins, New York, 1967); D. Altman and M. Farber, *Progress Report 9-26* (Jet Propulsion Laboratory, Pasadena, Calif., 1948).
19. A. Goldman, D. Murcray, F. Murcray, G. Cook, J. Van Allen, F. Bonomo, R. Blatherwick, *Geophys. Res. Lett.* **6**, 609 (1979).
20. I thank F. Fehsenfeld, J. Margitan, R. Hampson, G. Ray, F. Rowland, R. Rasmussen, and R. Watson for useful discussions and S. Walters for expert programming. Supported under NSF grant ATM78-26728; the National Center for Atmospheric Research (NSF-supported) provided support for computer time.

8 March 1979; revised 24 May 1979

Deciphering the Scattering Code Contained in the Resonance Echoes from Fluid-Filled Cavities in Solids

Abstract. *From the echoes of elastic waves incident on inclusions in solids, one may extract certain resonance features. These "spectral lines" and their widths form a code identifying the material composition of the inclusion in a way that resembles spectroscopy. This idea finds applications in geophysics, materials science, and any field dealing with materials containing inclusions.*

The amplitudes of backscattered waves returned by inclusions in viscoelastic solids, when plotted as a function of frequency, exhibit so many rapid oscillations and complicated features that until very recently it was not possible to extract the physical information contained in them. The amplitudes of these waves can be analyzed in light of our new resonance theory of scattering from cavities in solids (*1, 2*) and can be used to identify, for a given shape of the cavity, the material composition of the filler substance. When a (spherical) filler is set into oscillation by elastic (say, compressional) waves incident upon it, a set of modal resonances (fundamental and overtones) gets excited in it; these resonances characterize the filler as if they were its signature. Since incident shear waves excite the same resonances in the filler, we will limit this analysis to incident compressional waves and we shall consider fluid fillers only. From the usual spectral plots of the backscattered wave amplitudes versus nondimensional frequency $x \equiv k_d a$, it is possible to obtain these resonances, which manifest themselves as narrow lines or wider "spikes" ($k_d = \omega/c_d$, where ω is the circular frequency of the incident wave, c_d is the speed of the compressional waves, and a is the cavity radius). These plots display a quantity which, for simplicity, we will call "the echo." The way the resonances of an unknown filler are thus being used for purposes of material discrimination resembles the way chemical elements are identified from their optical spectra. The resonances obtained from the (heretofore physically incomprehensible) echo plot lead directly to a deciphering of the code, indicating the composition of the filler material that is contained in the echo.

Plane p (that is, compressional) elastic waves incident on fluid-filled spherical cavities in solids produce two scattered waves, one compressional and the other shear (that is, s). The scattering amplitudes f^{pp} or f^{ps} of both these scattered waves could be analyzed, but, since all the main points of this report can be shown from either one of these, we choose $f^{pp}(\theta)$. This nonmode-converted, normalized amplitude can be shown (*1*) to be

$$\frac{f^{pp}(\theta)}{a} = \sum_{n=0}^{\infty} \frac{f_n^{pp}(\theta)}{a} = \sum_{n=0}^{\infty} \frac{(2n+1)}{ik_d a} A_n P_n(\cos\theta) \qquad (1)$$

where the coefficients A_n are given by ratios of two 3×3 determinants whose elements contain products of the filler-to-matrix density ratio (that is, ρ_f/ρ) with various spherical Bessel and Hankel functions and their derivatives, of arguments $k_d a$ and $k_s a$, and of order n. These elements are determined from the boundary conditions of the problem and are given in (*1*). In the backscattering direction $\theta = \pi$, the Legendre polynominals are simplified by means of the relation $P_n(\cos\pi) = (-1)^n$. Figure 1 shows the plot of the modulus of this summed backscattered amplitude for a cavity filled with ethyl alcohol in an aluminum matrix. This is the "echo" containing the rapid oscillations and complex features mentioned above.